Available online at www.sciencedirect.com
ScienceDirect
Biochimica et Biophysica Acta 1773 (2007) 1619–1627
Biochimica et Biophysica Acta BBA
www.elsevier.com/locate/bbamcr

NEDD8: A new ataxin-3 interactor

Anabela Ferro [a,b], Ana Luísa Carvalho [c,d], Andreia Teixeira-Castro [e], Carla Almeida [d], Ricardo J. Tomé [f], Luísa Cortes [d], Ana-João Rodrigues [e], Elsa Logarinho [e], Jorge Sequeiros [a,b], Sandra Macedo-Ribeiro [f], Patrícia Maciel [e,*]

[a] *UnIGENe-IBMC, Instituto de Biologia Molecular e Celular, University of Porto, 4150-180 Porto, Portugal*
[b] *Institute of Biomedical Sciences Abel Salazar, University of Porto, 4099-003 Porto, Portugal*
[c] *Department of Zoology, University of Coimbra, 3004-517 Coimbra, Portugal*
[d] *Centre for Neuroscience and Cell Biology, University of Coimbra, 3004-517 Coimbra, Portugal*
[e] *Life and Health Sciences Research Institute (ICVS), School of Health Sciences, University of Minho, Campus de Gualtar, 4710-057 Braga, Portugal*
[f] *Molecular Structure Group-IBMC, Instituto de Biologia Molecular e Celular, Porto, Portugal*

Received 2 February 2007; received in revised form 13 July 2007; accepted 23 July 2007
Available online 24 August 2007

Abstract

Machado–Joseph disease (MJD/SCA3) is an autosomal dominant neurodegenerative disease caused by the expansion of a CAG tract in the coding portion of the *ATXN3* gene. The presence of ubiquitin-positive aggregates of the defective protein in affected neurons is characteristic of this and most of the polyglutamine disorders. Recently, the accumulation of the neural precursor cell expressed developmentally downregulated 8 (NEDD8), a ubiquitin-like protein, in the inclusions of MJD brains was reported. Here, we report a new molecular interaction between wild-type ataxin-3 and NEDD8, using in vitro and in situ approaches. Furthermore, we show that this interaction is not dependent on the ubiquitin-interacting motifs in ataxin-3, since the presence of the Josephin domain is sufficient for the interaction to occur. The conservation of the interaction between the *Caenorhabditis elegans* ataxin-3 homologue (atx-3) and NEDD8 suggests its biological and functional relevance. Molecular docking studies of the NEDD8 molecule to the Josephin domain of ataxin-3 suggest that NEDD8 interacts with ataxin-3 in a substrate-like mode. In agreement, ataxin-3 displays deneddylase activity against a fluorogenic NEDD8 substrate.

Keywords: Polyglutamine; UBL; Ubiquitin; E3 ligase; Neurodegeneration; MJD/SCA3

1. Introduction

Machado–Joseph disease (MJD/SCA3) is the most common dominantly inherited cerebellar ataxia worldwide [1]. The disease is caused by the expansion of a CAG repeat in the coding region of the gene *ATXN3*. This gene encodes ataxin-3 (ATXN3), a 42-kDa ubiquitously expressed protein, which has the polyglutamine tract located in the C-terminal region [2,3]. The repeat segment that normally consists of 12–44 CAG is expanded from 61 up to 87 in patients [4]. A striking feature of the polyglutamine diseases is the presence of neuronal inclusions in the affected brain regions; in MJD, the inclusions are both nuclear and cytoplasmic and typically ubiquitylated [5]. These intracellular inclusions contain proteasome subunits and chaperones, which suggests an attempt of the cell to either reduce the amount of non-native protein and restore protein homeostasis or eliminate the inclusions [6]. The physiological role of ATXN3 is not yet established.

Recently, it was noticed that the Josephin domain of ATXN3 (JD) contains conserved amino acids reminiscent of the catalytic domain of a member of the deubiquitylating cysteine protease UCH family (ubiquitin C-terminal hydrolases) [7] and later, in vitro assays showed that ATXN3 displays Ub hydrolase activity [8–10]. Strikingly, it was found that ATXN3 suppresses polyglutamine neurodegeneration in *Drosophila*, and this suppressing activity is dependent on its interaction with

Abbreviations: AMC, 7-amido-4-methylcoumarin; Ub, ubiquitin; UIM, ubiquitin-interacting motif; UBL, ubiquitin-like protein; UPS, ubiquitin–proteasome system; Y2H, yeast two-hybrid; SCF, SKP1-Cul-1-F-box protein E3

* Corresponding author. Tel.: +351 253 60 48 24; fax: +351 253 60 48 31.
E-mail address: pmaciel@ecsaude.uminho.pt (P. Maciel).

0167-4889/$ - see front matter © 2007 Elsevier B.V. All rights reserved.
doi:10.1016/j.bbamcr.2007.07.012

ubiquitin and on its protease activity [11]. Recent data showed the presence of neural precursor cell expressed developmentally downregulated gene 8 (NEDD8), an ubiquitin-like protein (UBL), in Ub-reactive neuronal and glial inclusions of several neurodegenerative diseases, namely MJD [12]. An active role was suggested for NEDD8 in the formation of the ubiquitylated inclusions through the ubiquitin–proteasome system (UPS). NEDD8 is the UBL with the highest structural homology with Ub [13] and conjugates to target proteins in a cascade of events similar to ubiquitylation [14]. So far, NEDD8 has been reported to conjugate with a limited number of target proteins, including the cullin family members [15] and p53 [16]. Cullins are the molecular scaffolds for the assembly of several E3 ubiquitin ligases, and the best known substrates for NEDD8 conjugation [15]. Neddylation upregulates the activities of cullin-organized E3 ubiquitin ligases while conferring intrinsic instability onto cullins [17]; thus, there is a close link between the ubiquitin and the NEDD8 pathways. NEDD8 deconjugation is equally important for the cell and can be carried out by members of most of the deubiquitylating enzyme (DUB) families UBP/USP (USP21), JAMM group (CNS/COP9 signalosome) and the ULP family (NEDP1/SENP8/DEN1) [18].

The fact that ATXN3 interacts with the UBL domain of HHR23 proteins [19] and the recent finding that NEDD8 is present in ubiquitylated inclusions in the brain of MJD patients led us to investigate whether ATXN3 could interact with NEDD8. In this study, we demonstrate in vitro and in situ that ATXN3 is able to establish a direct interaction with NEDD8, through its Josephin domain (JD). Interestingly, the *Caenorhabditis elegans* homologue of ATXN3, atx-3, also interacts with NEDD8, indicating that this protein interaction is evolutionarily conserved and, thus, of functional relevance. Furthermore, ATXN3 is able to cleave a fluorogenic substrate, NEDD8-AMC, which indicates that ATXN3 also has deneddylase activity.

2. Materials and methods

2.1. Antibodies

Primary antibody against ataxin-3 variant MJD1-1 (Swiss Prot no. P54252-2 VSP_002784) was raised in rabbits, by immunization with normal full-length recombinant 6His-ATXN3-var1.1, anti-MJD1.1 (David Biotechnologies). Competition assays were performed to verify the antibody specificity (Fig. S4).

2.2. Yeast two-hybrid assays

The yeast strain Y190 (96400) was purchased from ATCC. The original vectors pAS1-2 and pACT2 (kindly provided by Dr. S. Elledge, Baylor College of Medicine) were converted into yeast two-hybrid Gateway® vectors $pAS1_G$ and $pACT2_G$, respectively, following the manufacturer's instructions (Invitrogen). The $pAS1_G$-ATXN3 var1.1 coding for normal ATXN3, $pAS1_G$-JD, $pACT2_G$-JD, $pAS1_G$-NEDD8, $pACT2_G$-NEDD8 plasmids were generated using the Gateway cloning system®. The pAS1-ATXN3 var2.1 (17Q) (Swiss-Prot no. P54252) and pAS1-ATXN3-2.1N were prepared using classical cloning techniques [20]. The yeast transformations were performed using the lithium acetate method [21]. Transformants of $pAS1_G$-JD, $pAS1_G$-ATXN3 var1.1 or pAS1-ATXN3-2.1N were grown on SC-WLH supplemented with 130, 140 or 170 mM of amino-1,2,3 triazole (AT), respectively; the remaining were grown on plates with 20 mM AT. The interaction between SNF1 and SNF4 encoded by pSE1112 and pSE1111, respectively, was used as positive control (kindly provided by Dr. S. Elledge, Baylor College of Medicine). Incubations were performed at 30 °C for 5 days. Colony-lift β-galactosidase filter assays were performed according to the manufacturer's instructions (Clontech).

2.3. Expression plasmids and recombinant proteins

GST-tagged proteins—for the generation of GST-NEDD8 protein, NEDD8 cDNA was amplified from a human brain cDNA library using *att*B1-NEDD8 (5′-GGGGACAAGTTTGTACAAAAAAGCAGGCTGGATGCTAATTAAAGTGAAGAC-3′) and *att*B2-NEDD8 (5′-GGGGACCACTTTGTACAAGAAAGCTGGGTCTCACTGCCTAAGACCACCTC-3′) primers. GST-221cATXN3 expression construct was obtained using $pAS1_G$-ATXN3 var1.1 plasmid as template and *att*B1-221cATXN3 (5′-GGGGACAAGTTTGTACAAAAAAGCAGGCTGGATGTTAGACGAAGATGAG-3′) and *att*B2-MJD1.1 (5′-GGGGACCACTTTGTACAAGAAAGCTGGGTCTTATTTTTTTCCTTCTGTTTT-3′) primers. The cDNA for human HHR23A was reverse transcribed from total RNA of HeLa cells extracted with Trizol (Invitrogen) using *att*B1-HHR23A (5′-GGGGACAAGTTTGTACAAAAAAGCAGGCTGGATGGCCGTCACCATCACGCTG-3′) and *att*B2-HHR23A (5′-GGGGACCACTTTGTACAAGAAAGCTGGGTCTCACTCGTCATCAAAGTTCTG-3′) primers; gene-specific sequences are underlined. RT-PCR reactions were performed with Superscript RT kit (Invitrogen) according to the manufacturer's instructions. The aforementioned PCR products were first cloned into pDONR201 or pDONR207 vectors and then transferred to pDEST15 using the Gateway cloning system (Invitrogen) [22] according to the supplier's instructions.

6His-tagged proteins—the bacterial constructs expressing 6His-tagged ATXN3-var1.1, 6His-atx-3 and 6His-tagged Josephin domain (JD) were obtained and expressed as described [23]. The 6His-D1 construct (Fig. 2a) was obtained by introducing a stop codon at position 787 in *ATXN3* cDNA using the QuikChange site-directed mutagenesis kit (Stratagene) and protein expression was carried out as described [23]. The eukaryotic plasmid 6His-NEDD8 was a gift from Dr. R. Hay, University of St. Andrews [16].

GFP-tagged constructs—the eukaryotic pEGFP-ATXN3 (28Q) encoding normal ATXN3 in fusion with GFP (N-terminal) was a gift of Dr. Henry Paulson, University of Iowa. To obtain the mammalian pEGFP-JD plasmid encoding the fusion protein GFP-JD, a stop codon was introduced at position 548 in *ATXN3* cDNA of the pEGFP-ATXN3 (28Q) using the QuikChange site-directed mutagenesis kit according to the manufacturer's instructions (Stratagene). All clones were confirmed by automated sequencing.

2.4. Purification of recombinant proteins

The expression of GST, GST-NEDD8 was induced in *Escherichia coli* strain BL21(DE3) (Invitrogen), whereas GST-221cATXN3 was expressed in BL21 (DE3)pLysS (Invitrogen), all with 1 mM IPTG. GST-HHR23A was expressed in BL21(DE3)-SI cells (Invitrogen) using 300 mM NaCl. The bacterial protein expressions were carried out for 3 h at 30 °C. All GST-tagged proteins were purified with glutathione-sepharose™ 4B beads (GE Healthcare) according to the manufacturer's instructions and eluted with 10 mM reduced glutathione in 50 mM Tris–Cl pH 8.

2.5. GST pull-down assay

The purified GST or GST-tagged proteins (2 μg) were incubated rotating for 1 h at 4 °C with 50 μl of glutathione-sepharose™ 4B beads in 500 μl of in vitro binding buffer (IBB) (50 mM Tris–Cl pH 7.5, 150 mM NaCl, 10% glycerol, 1% Triton X-100, 1 mM EDTA, 1 mM DTT, 1 mM PMSF [24]). The 6His-J1, 6His-D1 or 6His-ATXN3-var1.1 was added and incubated for 1–2 h at 4 °C on a rotator. Incubations of 6His-ATXN3-var1.1, 6His-NEDD8 (UW9225, BioMol) or 6His-atx-3 were performed with 1% or 3% of BSA, respectively. Bound fractions were washed with IBB without glycerol and BSA, eluted by boiling in 50 μl of 2× SDS sample buffer and then were analysed by SDS-PAGE. Immunoblottings were performed using goat anti-GST (1:7500, GE Healthcare), mouse anti-6His (1:2000, Qiagen) or rabbit anti-MJD1.1 (1:25000) antibodies, all diluted in 1% SM/TBS-T (1% skimmed milk in Tris-buffered saline 1× (TBS), 0.05% Tween 20), or with rabbit anti-303JSP (1:2000)

antibody [25] or rabbit anti-NEDD8 (1:200), diluted in 3% SM/TBS-T. Secondary HRP-coupled antibody incubations were as follows: anti-goat 1:30,000, anti-mouse (Santa Cruz Biotechnology) both at 1:10,000 1% SM/TBS-T and anti-rabbit (Santa Cruz Biotechnology) 1:25,000 1% SM/TBS-T for ATXN3-var1.1 or 1:20,000 3% SM/TBS-T for atx-3. Detection was carried out with ECL (GE Healthcare).

2.6. Cell culture and transfection

HeLa cells were grown (37 °C, 5% CO_2) in DMEM (10938, GIBCO) supplemented with 10% of FBS, 100 U/ml penicillin, 4 mM glutamine and 500 μg/ml streptomycin (Gibco BRL). Cells were transfected at 70% cell confluence (5 μg of each expression plasmid) using Lipofectamine 2000 (Invitrogen) following the manufacturer's instructions and rinsed with PBS 8 h later; the DNA concentration was measured by spectrophotometer. Forty-eight hours after transfection whole cell protein extracts were prepared in 250 μl of lysis buffer [buffer A (50 mM Tris–HCl pH7.5, 150 mM NaCl, 0.5% Tween 20, 1 mM PMSF) plus 1 mM imidazole] supplemented with EDTA-free protease inhibitors cocktail (Roche). After sonication lysates were cleared by centrifugation and incubated with 50 μl of Ni-NTA agarose beads in lysis buffer. Beads were washed three times with washing buffer (buffer A plus 30 mM imidazole) and bound fractions were eluted with 50 μl of elution buffer (buffer A plus 500 mM imidazole). Eluted proteins were subjected to SDS-PAGE and immunoblotted with rabbit anti-GFP antibody at 1:2000 1% SM/TBS-T overnight, 4 °C. Detection was carried out with ECL detection kit.

2.7. Immunofluorescence and immunoprecipitation

For immunolocalization of endogenous ATXN3 and NEDD8, HEK293 cells were grown on coverslips and were fixed for 20 min in freshly prepared 4% *p*-formaldehyde (Sigma) in phosphate-buffered saline (PBS), permeabilized with PBS/0.1% Triton X-100 for 5–7 min, washed in PBS and blocked with PBS/10% FBS. ATXN3 was detected with anti-SCA3 (1H9 clone, Chemicon) at 1:500 and NEDD8 was detected with rabbit anti-NEDD8 (PW9340, BioMol) at 1:50. Fluorescent secondary antibodies (AlexaFluor 488-coupled goat anti-rabbit and AlexaFluor 568-coupled goat anti-mouse, Molecular probes) were used at 1:1500. DNA was stained with Dapi (Sigma). Images captured were then prepared and analysed using Photoshop 5.0LE (Adobe). For immunoprecipitation, HEK293 cells (CRL-1573, ATCC) were transfected with 10 μg of GFP-NEDD8 using Lipofectamine 2000 reagent (Invitrogen) following the manufacturer's instructions; cells were collected 48 h after transfection, lysed in buffer A plus 1 mM EDTA and protease inhibitors (Roche), briefly sonicated and cleared by centrifuged. The lysates were then pre-cleared with Protein-G-Sepharose (GE Healthcare) for 1 h at 4 °C and then incubated with 9 μl of polyclonal anti-NEDD8 antibody (PW9340) overnight at 4 °C. The immunocomplexes were precipitated with Protein-G-Sepharose at 4 °C for 2 h; the beads were washed two times with buffer A minus the detergent and finally eluted with 2× SDS sample buffer. The eluted proteins were analysed by Western blot with anti-SCA3 (1H9) or anti-GFP.

2.8. Molecular docking prediction

Models of the JD-NEDD8 and of JD–ubiquitin complexes were built by superimposing the structures of the NED1–NEDD8 complex (PBD ID 1xt9 [26]) and of the UCH-L3 ubiquitin vinylmethylesther complex (PDB ID 1xd3 [27]), respectively, with the JD domain (PDB ID 1yzb [10]) using the DALI server [28]. The structures superpose with JD with *Z*-scores of 1.8 and 4.5, and rmsds of 3.4 and 2.9 Å, respectively. The interface between the two proteins in the docked complexes was further refined by geometry optimization with CNS [29]. All images were made with PyMOL (http://pymol.sourceforge.net/).

2.9. NEDD8-AMC cleavage assay

The putative deneddylase activity of the proteins was evaluated using the fluorogenic substrate NEDD8-AMC, a reagent that allows determination of NEDD8 C-terminal hydrolase activity, according to a previously described protocol [30]. Briefly, 300 μl of assay buffer (50 mM HEPES, 0.5 mM EDTA, pH 7.5, with 0.1 mg/ml BSA and 1 mM DTT) containing 10 μg of ATXN3 or ATXN3C14A, purified as described [23], was incubated at 37 °C for 30 min. The reaction was initiated by adding the substrate to a final concentration of 0.5 μM and the proteins' hydrolytic activities were measured as the release of AMC, after cleavage, for 9 min using a Perkin Elmer LS 50B fluorimeter.

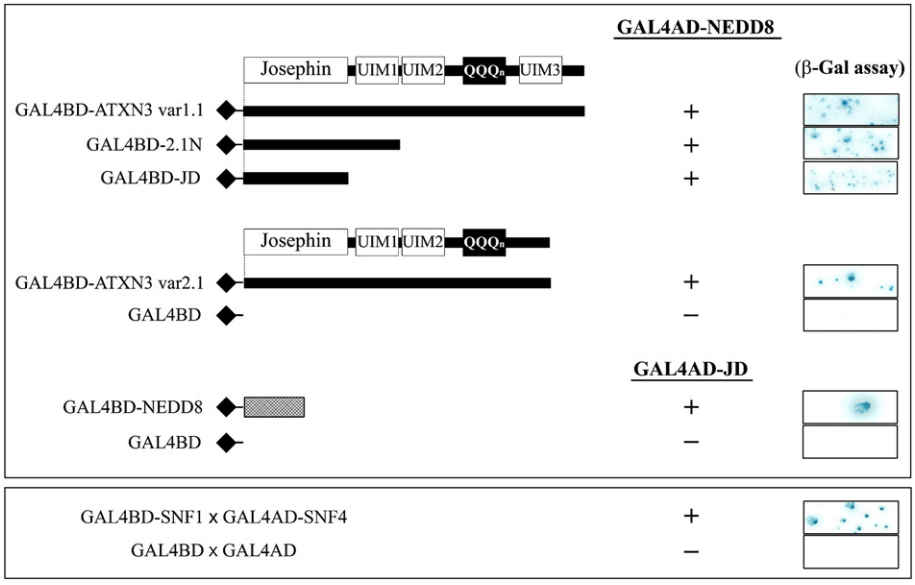

Fig. 1. ATXN3 interacts with NEDD8 in the yeast two-hybrid system. The schematic representation depicts all yeast expression plasmids used. Two cDNA variants encoding normal ataxin-3 were used: GAL4BD-ATXN3 var1.1 and GAL4BD-ATXN3 var2.1, which lacks UIM3. Two constructs comprising fragments of ATXN3 were also tested: $pAS1_G$-JD encodes GAL4BD fusion to Josephin domain and pAS1-2.1N encodes JD plus functional UIM1. The reverse interaction between GAL4BD-NEDD8 (crossed rectangle) and GAL4AD-JD was also tested; the filled rhombus represents the GAL4BD tag. An interaction was considered positive (+) when growth on nutritional selection plates was observed and colonies stained blue when tested for β-galactosidase expression (β-Gal assay).

3. Results and discussion

3.1. ATXN3 interacts with NEDD8

In order to evaluate if ATXN3 interacts with NEDD8, we used the yeast two-hybrid system (Y2H) and GST pull-down assays. For this study, several Y2H constructs of ATXN3 were made, coding for the entire protein (Gal4BD-ATXN3 var1.1), the JD (Gal4BD-JD) or the JD plus the first UIM (ubiquitin-interacting motif) (Gal4BD-2.1N). A second variant of ATXN3, ATXN3 var2.1, in which UIM3 is absent, was also tested (see W-S1). The results showed that ATXN3 interacts with NEDD8, in the Y2H assay (Fig. 1). No difference was observed when isoform ATXN3 var1.1 or ATXN3 var2.1 was tested, indicating that the third UIM in ATXN3 does not influence its ability to interact with NEDD8. To pinpoint the region in ATXN3 responsible for the interaction with NEDD8, two truncated fragments of ATXN3 were tested (Fig. 1). The results obtained with the different fragments of ATXN3 showed that the JD is sufficient to establish the interaction with NEDD8. We tested also the reverse interaction between GAL4BD-NEDD8 and GAL4AD-JD and a positive interaction was observed. Co-transformations of the bait or prey constructs with the pACT2 and pAS1 Y2H empty vectors, respectively, showed no positive interactions (Fig. 1). The results obtained with the Y2H analysis were confirmed using in vitro pull-down assays, by monitoring the binding of GST-NEDD8 to several 6His-tagged constructs of ATXN3 (Fig. 2a). As shown in Fig. 2b, full-length ATXN3 interacts in vitro with NEDD8, further indicating that ATXN3 can bind NEDD8 directly. In order to evaluate whether the interaction between ATXN3 and NEDD8 is evolutionarily conserved, we tested if the *C. elegans* atx-3 could also interact with human NEDD8. Interestingly, we observed a positive interaction between human NEDD8 and atx-3 protein (Fig. 2c). The high degree of JD conservation, despite an overall identity of only 36% between atx-3 and human ATXN3, may explain this direct interaction (see W-S1). In *C. elegans*, ned-8 has been shown to be crucial for nematode development. The absence of ned-8 resulted in embryonic lethality or severe developmental abnormalities [31]. The conservation of the atx-3/NEDD8 interaction throughout evolution suggests a biological and functional relevance for this protein pair. As a control experiment, we tested

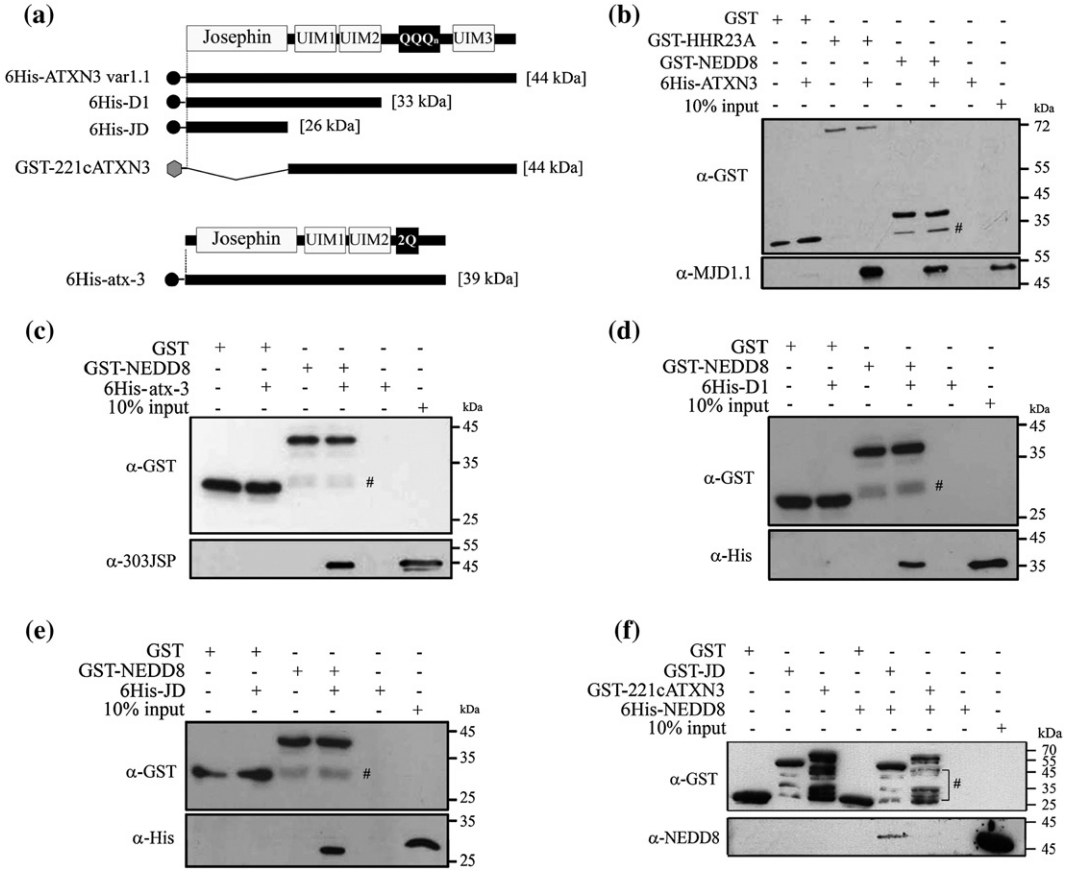

Fig. 2. ATXN3 interacts with NEDD8 in vitro. The GST pull-down assays show direct interaction of ATXN3 with NEDD8. (a) Schematic representation of recombinant proteins used in the assays: 6His-ATXN3 var1.1 represents the full-length of ataxin-3 variant 1.1 with three UIMs; 6His-D1 comprises the JD plus two UIMs; 6His-JD comprises only the JD; GST-221cATXN3 comprises all domains of ATXN3 var1.1 except JD, and 6His-atx-3 represents the ataxin-3 of *C. elegans*. Expected molecular weights for all proteins are stated (brackets). Purified GST-NEDD8 was incubated with ATXN3 full-length (b), 6His-D1 (d), 6His-JD (e) or atx-3 (c); GST-221cATXN3 was incubated with 6His-NEDD8 (f). Interaction between GST-HHR23A and 6His-ATXN3 was observed under the conditions established (b). Input lanes show 10% of the 6His-tagged protein used in the assay. NEDD8 pulled-down ATXN3 (b), its fragments 6His-D1 (d) and 6His-JD (e) and atx-3 (c), but failed to interact with GST-221cATXN3. GST alone showed no binding in any assay. Bands identified with cardinals (#) are protein degradation products.

the interaction between ATXN3 and HHR23A (Fig. 2b), and under the conditions used, we were able to replicate the interaction reported before [19]. Our results also suggest that ATXN3 is able to interact more efficiently with NEDD8 and HHR23A, than with monomeric Ub (Fig. S2), since a higher amount of GST-Ub was needed to pull-down a quantity of ATXN3 similar to those obtained with NEDD8 and HHR23A (Fig. 2b, d). We also mapped the minimum domain required for ATXN3 to interact with NEDD8 using the pull-down assays. Truncated fragments of ATXN3 corresponding to the JD plus UIM1 and UIM2 (6His-D1), the JD alone (6His-JD) or a C-terminal fragment comprising all ATXN3 domains except JD (GST-221c ATXN3) were produced and assayed for binding to NEDD8. We did observe interaction between GST-NEDD8 and 6His-D1 or 6His-JD proteins (Fig. 2d, e), but no interaction was observed between GST-221cATXN3 and 6His-NEDD8. Thus, we conclude that the JD of ATXN3 is sufficient and necessary for the interaction with NEDD8, in agreement with the results obtained in the Y2H assay (Fig. 1). No interactions between the D1 or JD fragments of ATXN3 and monomeric Ub were observed in these in vitro studies (Fig. S2b, c). In control experiments we could not detect any binding of ATXN3 or its truncated forms to the beads alone, or to beads containing GST, indicating that the interactions observed with NEDD8 are specific (Fig. 2b–f). Taken together, the results obtained, using the Y2H system and GST pull-down assays, indicate that ATXN3 interacts with NEDD8 through its JD.

3.2. ATXN3 and NEDD8 colocalize and interact in mammalian cells

The subcellular expression of endogenous ATXN3 and NEDD8 proteins was determined in HeLa cells, using immunofluorescence analysis. Cells were fixed, permeabilized and then immunolabelled with anti-SCA3 (1H9 clone) and anti-NEDD8 (PW9340) antibodies. Both proteins have nuclear and cytoplasmic diffuse distribution (Fig. 3a). Incubations with secondary antibodies alone did not produce specific staining (data not shown). Merged images show colocalization of ATXN3 and NEDD8, both in the nucleus and cytoplasm, which is compatible with the possibility that the two proteins are interacting partners.

In order to investigate whether ATXN3 can bind NEDD8 in the context of a mammalian cell, the interaction was analysed in transfected HeLa cells. Briefly, 6His-NEDD8 was co-expressed either with GFP-JD or GFP alone (Fig. 3b). His-tagged proteins were purified under non-denaturing conditions, and the purified samples were subsequently immunoblotted with an anti-GFP

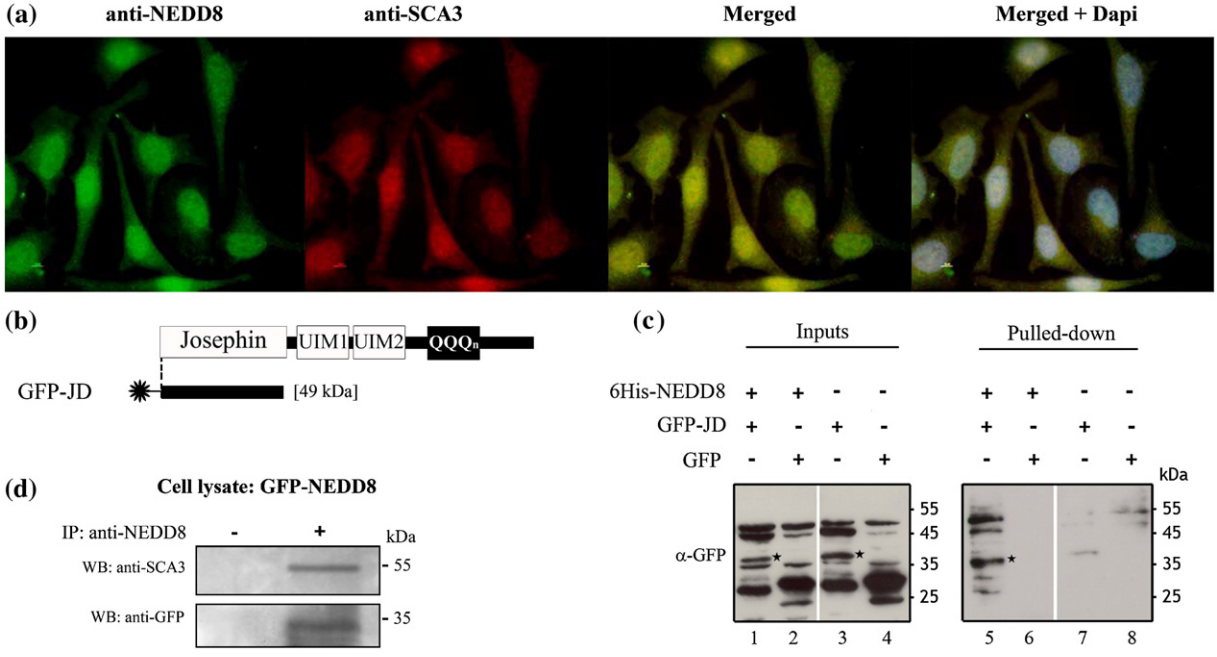

Fig. 3. Ataxin-3 interacts with NEDD8 in eukaryotic cells. (a) Immunofluorescence analysis showed nuclear and cytoplasmatic colocalization of endogenous ATXN3 and NEDD8. Localization of ATXN3 was detected with anti-SCA3 (1H9) antibody and probed with AlexaFluor 568-coupled goat anti-mouse secondary antibody (red); detection of NEDD8 was performed with polyclonal anti-NEDD8 antibody and revealed by AlexaFluor 488-coupled goat anti-rabbit fluorescent antibody (green); nuclei were stained with Dapi (Sigma). (b) Schematic representation of the N-terminal GFP-tagged eukaryotic expression plasmid (GFP-JD) used in mammalian cell transfection; the expected molecular weight of GFP-JD fusion protein is stated (brackets); filled star represents the GFP tag. (c) ATXN3 interacts with NEDD8 in mammalian cells. The 6His-NEDD8 was co-expressed with GFP-JD (lanes 1, 5) or empty vector (lanes 2, 6) in HeLa cells. Single expressions of GFP-JD (lane 7) or GFP alone (lane 8) were used as control assays. Lanes 1–4 were loaded with 5% of the total protein input of each assay. GFP-JD pulled-down by 6His-NEDD8 (black star) was detected by Western blotting using the anti-GFP antibody (SC-8334, Santa Cruz Biotechnology). (d) Endogenous ATXN3 is immunoprecipitated by GFP-tagged NEDD8. Cells expressing GFP-NEDD8 were harvested and the supernatants pre-cleared with protein-G-sepharose beads. Supernatants were then incubated overnight with anti-NEDD8 antibody (+) or without the antibody (−); immunocomplexes were subsequently separated by SDS-PAGE and immunoblotted with anti-SCA3 or anti-GFP antibodies.

antibody (Fig. 3c). Cells transfected only with pEGFP-JD or pEGFP were used as controls. The interaction of 6His-NEDD8 with the JD (Fig. 3c, lane 5) was detected in this assay supporting the previous results. No binding of GFP alone to NEDD8 was detected (Fig. 3c, lane 6), indicating that ATXN3 and JD fusion proteins were specifically co-purified with NEDD8. It should be noted that the purified proteins detected using the anti-GFP antibody have molecular sizes corresponding to unmodified GFP-JD, suggesting that ATXN3 is not neddylated, but rather that it interacts with NEDD8.

To further confirm the occurrence of this new interaction in vivo, HEK293 cells were transiently transfected with a construct expressing GFP-NEDD8. When the cell lysates were incubated with polyclonal anti-NEDD8 we were able to co-immunoprecipitate the endogenous ATXN3 (Fig. 3d). No ATXN3 was detected in the negative control (omission of the anti-NEDD8 antibody). An immunoblot assay with anti-GFP confirmed that GFP-NEDD8 protein was efficiently immunoprecipitated (Fig. 3d). Altogether, these results suggest that endogenous ATXN3 specifically interacts with NEDD8.

Costa et al. [32] reported the expression pattern of murine ATXN3, which is expressed ubiquitously since early embryonic stages, at least in E11.5. Interestingly, previous mRNA studies showed that the highest expression of the NEDD8 message

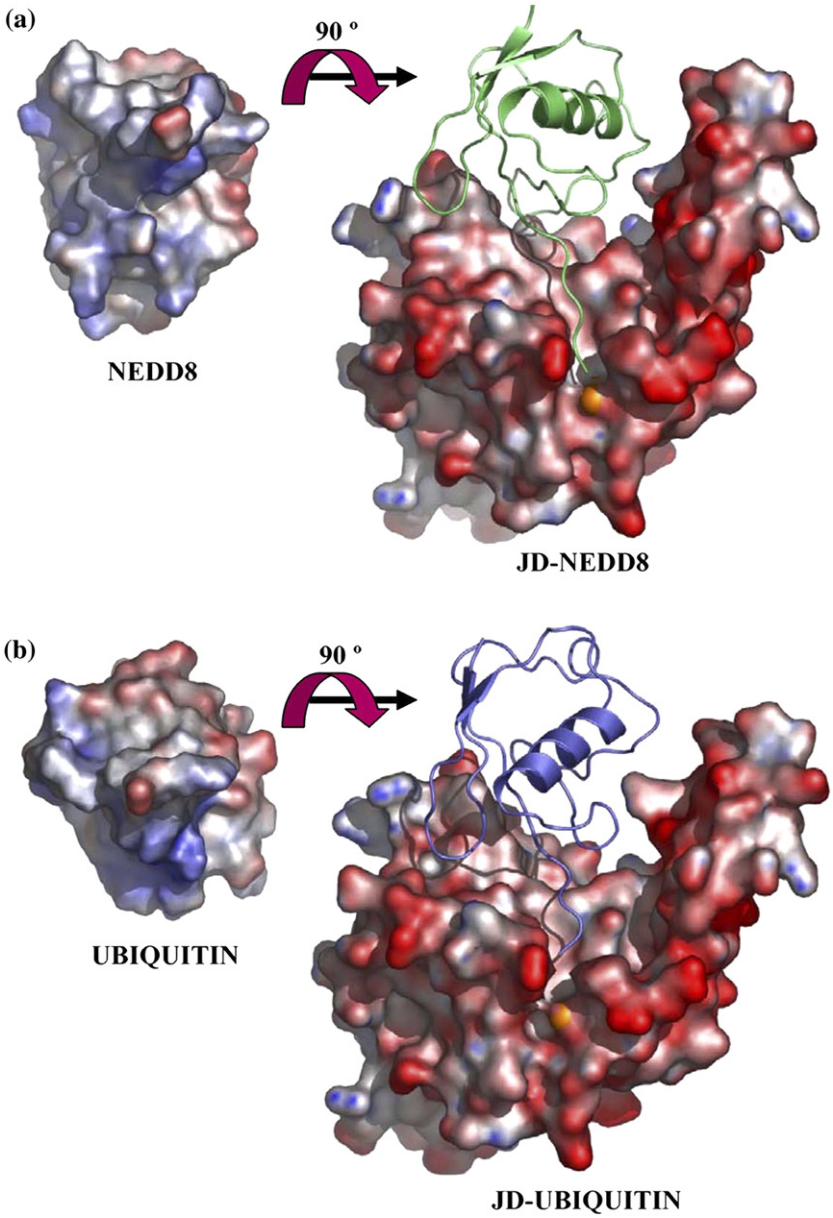

Fig. 4. NEDD8 and ubiquitin share the same binding site on ATXN3 catalytic domain. Solid surface representation of the JD, NEDD8 and Ub coloured according to the electrostatic potential (blue for positive, red for negative). JD is complexed (a) with NEDD8 (green) and (b) with Ub (violet). The pictures on the left of panels a and b show solid surface representations of NEDD8 and Ub rotated ~90° along the horizontal axis in the figure plane, in comparison with their position in the docked complex. The docking surfaces of NEDD8 and Ub are predominantly basic and complement the acidic character of the substrate-binding cleft of the JD. The overall surface complementarity is notorious in both complexes.

occurs at the E11 stage; moreover, Kamitani et al. [33] have proposed that proteins expressed in the heart and skeletal muscle or in early development would be good candidates for NEDD8 interaction. Strikingly, mouse ATXN3 shows prominent expression in these particular tissues [32]. All these data support a biological relevance for the ATXN3/NEDD8 interaction, not only in differentiated tissues, but also since early stages of development.

3.3. NEDD8 interacts with ATXN3 in a substrate-like mode

Recently, the structure of JD of ATXN3 has been determined by NMR [10,34], revealing that it shares a significant structural homology with the DUB enzymes, human UCH-L3 [27] and yeast YUH1 [35]. Those studies allowed mapping of the active site (Q9, C14, H119, N134) and revealed that the binding site for the N-terminal UBL domain of HHR23B is comprised of an hydrophobic surface located opposite to the catalytic site of the JD [10]. The binding site of Ub as a substrate has been proposed to be located just above the active site, in a cleft bordered by the central catalytic subdomain and by a flexible helical hairpin that is likely to move to better accommodate the substrate [10,34]. Our data show that ATXN3 interacts specifically with NEDD8, and that the interaction site involves its catalytic JD. The high sequence and structural similarity between NEDD8, Ub and the UBL domain of HHR23B raises two possible scenarios: (i) NEDD8 could interact with ATXN3 JD via its exposed hydrophobic surface used for the HHR23B interaction [10] or (ii) NEDD8 could interact with ATXN3 in a substrate-like mode, meaning that ATXN3 could have deneddylase activity.

We have analysed the surface distribution of conserved and divergent residues between the UBL domain of HHR23B and NEDD8, and between Ub and NEDD8, in an effort to identify the structural basis of their differential binding to ATXN3. The hydrophobic HHR23B-UBL surface relevant for the interaction with the JD is not strictly conserved in NEDD8 and we can predict that the NEDD8 interaction site on the JD is likely to be different. We predict that NEDD8 interacts with the JD in a substrate-like manner. Our docking model of Ub and NEDD8 at the putative substrate-binding site of the JD was built based on the structural homology between Ub/NEDD8 hydrolases and JD. For both complexes the C-terminus-GG76 motif, common to NEDD8 and Ub, is bound deep in the narrow catalytic canyon, close to the catalytic C14 of ATXN3 (Fig. 4). Accommodation of either NEDD8 or Ub involves small structural changes both in the JD and in the docked molecules (data not shown), in regions that have been shown, by chemical shift perturbation, to be relevant for the JD–ubiquitin interaction [34]. In these models, the negative electrostatic surface potential of the JD is complemented by the positive charge of the docked molecules (Fig. 4a and b) and docking is further aided by surface complementarity. Our modelling studies clearly show that both NEDD8 and Ub should bind in a substrate-like mode. In agreement, ATXN3 has NEDD8 C-terminal hydrolase activity against the fluorogenic substrate NEDD8-AMC (7-amido-4-methylcoumarin)

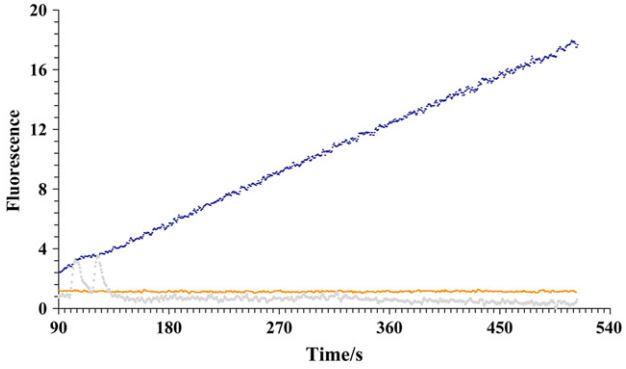

Fig. 5. Hydrolysis of NEDD8-AMC by ATXN3 requires the C14 residue. ATXN3 displays C-terminal hydrolase activity against NEDD8-AMC (Boston Biochemicals). Recombinant ATXN3 or mutant ATXN3 (ATXN3C14A) was incubated with NEDD8-AMC (7-amido-4-methylcoumarin) for a total of 9 min, and their deneddylase activities measured from the AMC release extent, after cleavage. No cleavage was observed when only the assay buffer was present (grey line) or the mutant ATXN3C14A (orange line). However, when ATXN3 was present in the reaction a time-dependent release of AMC could be observed (blue line) indicating the hydrolytic activity of ATXN3 on NEDD8-AMC. The slope for the ATXN3 and ATXN3C14A activities were 0.037 s^{-1} and 0.0032 s^{-1}, respectively.

(Fig. 5). Furthermore, our results clearly show that the deneddylase activity of ATXN3 is dependent on the cysteine at position 14. The mutant ATXN3 (C14A) does not show deneddylase activity against NEDD8-AMC (Fig. 5). However, this activity loss is not due to loss of interaction between these proteins since NEDD8 is still able to interact with mutant ATXN3 JD(C14A) (see Fig. S3).

In conclusion, in this study, we identified a novel molecular partner of ATXN3, NEDD8. We demonstrated that the interaction between NEDD8 and ATXN3 is specific and independent of the presence of the UIM domains and the polyglutamine tract, since it occurs through its JD. In contrast, interaction with monomeric Ub is weaker and it requires the full-length protein. The specific interaction between the JD and NEDD8 prompted us to build a theoretical model of the complex, which shows that monomeric Ub and NEDD8 could share the same binding site. Moreover, we show that ATXN3 has a deneddylase activity dependent on the cysteine residue at position 14.

The NEDD8 protein is essential for the activity of SCF-like ubiquitin ligase complexes. These complexes determine the degradation of several substrates and consequently pace the pathways in which they participate. Our group has recently reported a transcriptomic analysis of *atx-3* knockout *C. elegans* strains [25] where we showed downregulation of several genes encoding subunits of the SCF complex. Additionally, a recent analysis of genetic interactions in *C. elegans* by Zhong and Sternberg [36] pinpointed several genes encoding UPS-related proteins and components of SCF-like complexes as genetic interactors of atx-3 in the worm. Together with these results, the identification of NEDD8 as a new ATXN3 interacting protein adds a new perspective to the possible physiological role of ATXN3 modulating the activity of the UPS.

Further studies will be needed to explore the nature and specificity determinants of this newly identified interaction, to clarify its physiological role and the biological relevance of the putative deneddylase activity of ATXN3.

Acknowledgments

We thank Dr. H. Paulson, Dr. R. Hay, Dr. D. Bohmann, Dr. S. Elledge and PM laboratory members for the reagents and assistance provided. A.F. would like to address special thanks to Carlos Melo for the continuous support, Maria do Carmo Costa and Sandra Santos for all the assistance with the Y2H and cell culture assays. This work was funded by FCT (POCTI/MGI/47550/2002; SAU-MMO 60412/2004; POCI/SAU-MMO/60156/2004), Fundação Luso-Americana para o Desenvolvimento (Proc.3.L/A.II/I P.582/99) and the National Ataxia Foundation. A.F. (SFRH/BD/1288/2000), A.T.-C. (SFRH/BI/11844/2003) and A.-J.R. (SFRH/BD/17066/2004) are scholarship recipients from FCT.

Appendix A. Supplementary data

Supplementary data associated with this article can be found, in the online version, at doi:10.1016/j.bbamcr.2007.07.012.

References

[1] L. Schols, P. Bauer, T. Schmidt, T. Schulte, O. Riess, Autosomal dominant cerebellar ataxias: clinical features, genetics, and pathogenesis, Lancet Oncol. 3 (2004) 291–304.
[2] Y. Kawaguchi, T. Okamoto, M. Taniwaki, M. Aizawa, M. Inoue, S. Katayama, H. Kawakami, S. Nakamura, M. Nishimura, I. Akiguchi, CAG expansions in a novel gene for Machado–Joseph disease at chromosome 14q32.1, Nat. Genet. 8 (1994) 221–228.
[3] T. Schmidt, G.B. Landwehrmeyer, I. Schmitt, Y. Trottier, G. Auburger, F. Laccone, T. Klockgether, M. Volpel, J.T. Epplen, L. Schols, O. Riess, An isoform of ataxin-3 accumulates in the nucleus of neuronal cells in affected brain regions of SCA3 patients, Brain Pathol. 8 (1998) 669–679.
[4] P. Maciel, M.C. Costa, A. Ferro, M. Rousseau, C.S. Santos, C. Gaspar, J. Barros, G.A. Rouleau, P. Coutinho, J. Sequeiros, Improvement in the molecular diagnosis of Machado–Joseph disease, Arch. Neurol. 58 (2001) 1821–1827.
[5] H.L. Paulson, M.K. Perez, Y. Trottier, J.Q. Trojanowski, S.H. Subramony, S.S. Das, P. Vig, J.L. Mandel, K.H. Fischbeck, R.N. Pittman, Intranuclear inclusions of expanded polyglutamine protein in spinocerebellar ataxia type 3, Neuron 19 (1997) 333–344.
[6] T. Schmidt, K. Lindenberg, A. Krebs, L. Schöls, F. Laccone, J. Herms, M. Rechsteiner, O. Riess, G. Landwehrmeyer, Protein surveillance machinery in brains with spinocerebellar ataxia type 3: redistribution and differential recruitment of 26S proteasome subunits and chaperones to neuronal intranuclear inclusions, Ann. Neurol. 51 (2002) 302–310.
[7] H. Scheel, S. Tomiuk, K. Hofmann, Elucidation of ataxin-3 and ataxin-7 function by integrative bioinformatics, Hum. Mol. Genet. 12 (2003) 2845–2852.
[8] B. Burnett, F. Li, R.N. Pittman, The polyglutamine neurodegenerative protein ataxin-3 binds polyubiquitylated proteins and has ubiquitin protease activity, Hum. Mol. Genet. 12 (2003) 3195–3205.
[9] S.J. Berke, Y. Chai, G.L. Marrs, H. Wen, H.L. Paulson, Defining the role of ubiquitin-interacting motifs in the polyglutamine disease protein, ataxin-3, J. Biol. Chem. 280 (2005) 32026–32034.
[10] G. Nicastro, R.P. Menon, L. Masino, P.P. Knowles, N.Q. McDonald, A. Pastore, The solution structure of the Josephin domain of ataxin-3: structural determinants for molecular recognition, Proc. Natl. Acad. Sci. U. S. A. 102 (2005) 10493–10498.
[11] J.M. Warrick, L.M. Morabito, J. Bilen, B. Gordesky-Gold, L.Z. Faust, H.L. Paulson, N.M. Bonini, Ataxin-3 suppresses polyglutamine neurodegeneration in *Drosophila* by a ubiquitin-associated mechanism, Mol. Cell 18 (2005) 37–48.
[12] F. Mori, M. Nishie, K. Wakabayashi, Y.S. Piao, H. Takahashi, K. Kito, T. Kamitani, Accumulation of NEDD8 in neuronal and glial inclusions of neurodegenerative disorders, Neuropathol. Appl. Neurobiol. 31 (2005) 53–61.
[13] F.G. Whitby, G. Xia, C.M. Pickart, C.P. Hill, Crystal structure of the human ubiquitin-like protein NEDD8 and interactions with ubiquitin pathway enzymes, J. Biol. Chem. 273 (1998) 34983–34991.
[14] M. Hochstrasser, Evolution and function of ubiquitin-like protein-conjugation systems, Nat. Cell Biol. 2 (2000) E153–E157.
[15] Z.Q. Pan, A. Kentsis, D.C. Dias, K. Yamoah, K. Wu, NEDD8 on cullin: building an expressway to protein destruction, Oncogene 23 (2004) 1985–1997.
[16] D.P. Xirodimas, M.K. Saville, J.C. Bourdon, R.T. Hay, D.P. Lane, Mdm2-mediated NEDD8 conjugation of p53 inhibits its transcriptional activity, Cell 118 (2004) 83–97.
[17] J.T. Wu, H.C. Lin, Y.C. Hu, C.T. Chien, Neddylation and deneddylation regulate Cul1 and Cul3 protein accumulation, Nat. Cell. Biol. 7 (2005) 1014–1020.
[18] G. Parry, M. Estelle, Regulation of cullin-based ubiquitin ligases by the NEDD8/RUB ubiquitin-like proteins, Semin. Cell Dev. Biol. 15 (2004) 221–229.
[19] G. Wang, N. Sawai, S. Kotliarova, I. Kanazawa, N. Nukina, Ataxin-3, the *MJD1* gene product, interacts with the two human homologs of yeast DNA repair protein RAD23, HHR23A and HHR23B, Hum. Mol. Genet. 9 (2000) 1795–1803.
[20] J. Sambrook, D. Russel, Molecular Cloning: A Laboratory Manual, Third ed.Cold Spring Harbor Laboratory Press, New York, 2001.
[21] R.D. Gietz, R.H. Schiestl, A.R. Willems, R.A. Woods, Studies on the transformation of intact yeast cells by the LiAc/SS-DNA/PEG procedure, Yeast 11 (1995) 355–360.
[22] J.L. Hartley, G.F. Temple, M.A. Brasch, DNA cloning using in vitro site-specific recombination, Genome Res. 10 (2000) 1788.
[23] L. Gales, L. Cortes, C. Almeida, C.V. Melo, M. do Carmo Costa, P. Maciel, D.T. Clarke, A.M. Damas, S. Macedo-Ribeiro, Towards a structural understanding of the fibrillization pathway in Machado–Joseph's disease: trapping early oligomers of non-expanded ataxin-3, J. Mol. Biol. 353 (2005) 642–654.
[24] H. Otera, T. Harano, M. Honsho, K. Ghaedi, S. Mukai, A. Tanaka, A. Kawai, N. Shimizu, Y. Fujiki, The mammalian peroxin Pex5pL, the longer isoform of the mobile peroxisome targeting signal (PTS) type 1 transporter, translocates the Pex7p-PTS2 protein complex into peroxisomes via its initial docking site, Pex14p, J. Biol. Chem. 275 (2000) 21703–21714.
[25] A.-J. Rodrigues, G. Coppola, C. Santos, M.d.C. Costa, M. Ailion, J. Sequeiros, D.H. Geschwind, P. Maciel, Functional genomics and biochemical characterization of the *C. elegans* orthologue of the Machado–Joseph disease protein ataxin-3, FASEB J. 21 (2007) 1126–1136.
[26] D. Reverter, K. Wu, T.G. Erdene, Z.Q. Pan, K.D. Wilkinson, C.D. Lima, Structure of a complex between NEDD8 and the Ulp/Senp protease family member Den1, J. Mol. Biol. 345 (2005) 141–151.
[27] S. Misaghi, P.J. Galardy, W.J.N. Meester, H. Ovaa, H.L. Ploegh, R. Gaudet, Structure of the ubiquitin hydrolase UCH-L3 complexed with a suicide substrate, J. Biol. Chem. 280 (2005) 1512–1520.
[28] L. Holm, J. Park, DaliLite workbench for protein structure comparison, Bioinformatics 16 (2000) 566–567.
[29] A.T. Brunger, P.D. Adams, G.M. Clore, W.L. DeLano, P. Gros, R.W. Grosse-Kunstleve, J.S. Jiang, J. Kuszewski, M. Nilges, N.S. Pannu, R.J. Read, L.M. Rice, T. Simonson, G.L. Warren, Crystallography & NMR system: a new software suite for macromolecular structure determination, Acta Crystallogr., D Biol. Crystallogr. 54 (Pt 5) (1998) 905–921.

[30] B.G. Burnett, R.N. Pittman, The polyglutamine neurodegenerative protein ataxin 3 regulates aggresome formation, Proc. Natl. Acad. Sci. U. S. A. 102 (2005) 4330–4335.
[31] D. Jones, E.P.M. Candido, The ned-8 conjugating system in *Caenorhabditis elegans* is required for embryogenesis and terminal differentiation of the hypodermis, Dev. Biol. 226 (2000) 152–165.
[32] M.C. Costa, J. Gomes-da-Silva, C.J. Miranda, J. Sequeiros, M.M. Santos, P. Maciel, Genomic structure, promoter activity, and developmental expression of the mouse homologue of the Machado–Joseph disease (MJD) gene, Genomics 84 (2004) 361–373.
[33] T. Kamitani, K. Kito, H.P. Nguyen, E.T.H. Yeh, Characterization of NEDD8, a developmentally down-regulated ubiquitin-like protein, J. Biol. Chem. 272 (1997) 28557–28562.
[34] Y. Mao, F. Senic-Matuglia, P.P. Di Fiore, S. Polo, M.E. Hodsdon, P. De Camilli, Deubiquitinating function of ataxin-3: insights from the solution structure of the Josephin domain, Proc. Natl. Acad. Sci. U. S. A. 102 (2005) 12700–12705.
[35] S.C. Johnston, S.M. Riddle, R.E. Cohen, C.P. Hill, Structural basis for the specificity of ubiquitin C-terminal hydrolases, EMBO J. 18 (1999) 3877–3887.
[36] W. Zhong, P.W. Sternberg, Genome-wide prediction of *C. elegans* genetic interactions, Science 311 (2006) 1481–1484.